PHOTONICS Research

Wideband tunable passively Q-switched fiber laser at 2.8 μm using a broadband carbon nanotube saturable absorber

YANJIA LÜ,[1,†] CHEN WEI,[1,5,†] HAN ZHANG,[2] ZHE KANG,[3,6] GUANSHI QIN,[4] AND YONG LIU[1]

[1]State Key Laboratory of Electronic Thin Films and Integrated Devices, School of Optoelectronic Science and Engineering, University of Electronic Science and Technology of China, Chengdu 610054, China
[2]College of Electrical Engineering and Information Technology, Sichuan University, Chengdu 610065, China
[3]Changchun Observatory, National Astronomical Observatories, Chinese Academy of Sciences, Changchun 130012, China
[4]State Key Laboratory on Integrated Optoelectronics, College of Electronic Science & Engineering, Jilin University, Changchun 130012, China
[5]e-mail: cwei@uestc.edu.cn
[6]e-mail: kangz@cho.ac.cn

Received 28 August 2018; revised 1 November 2018; accepted 2 November 2018; posted 2 November 2018 (Doc. ID 344330); published 7 December 2018

We propose and demonstrate a widely tunable passively Q-switched Ho^{3+}/Pr^{3+}-codoped ZrF_4-BaF_2-LaF_3-AlF_3-NaF fiber laser operating in the 2.8 μm mid-infrared (MIR) waveband based on a single-walled carbon nanotube (SWCNT) saturable absorber (SA). The SWCNTs have diameters ranging from 1.4 to 1.7 nm. The modulation depth and saturation intensity of the SWCNT SA measured at 2850 nm are 16.5% and 1.66 MW/cm^2, respectively. Stable Q-switched pulses with the shortest pulse duration of 1.46 μs and the maximum pulse energy of 0.43 μJ are achieved at a launched pump power of 445.6 mW. The combined use of a broadband SWCNT SA and a plane ruled grating ensures a broad continuously tuning range of 55.0 nm from 2837.6 to 2892.6 nm. The output powers, emission spectra, repetition rates, and pulse durations at different tuning wavelengths are also characterized and analyzed. Our results indicate that SWCNTs can be excellent broadband SAs in the 3 μm MIR region. To the author's knowledge, this is the first demonstration of a widely tunable carbon-nanotube-enabled passively Q-switched fiber laser operating in the 2.8 μm MIR waveband.

https://doi.org/10.1364/PRJ.7.000014

1. INTRODUCTION

Mid-infrared (MIR) wavelength-tunable pulsed fiber lasers emitting at around 3 μm are desirable sources in a diverse range of applications such as atmospheric pollution monitoring, non-invasive diagnostics, and nonlinear optical systems [1–5]. Currently, the dominant pulse generation approaches in the ~3 μm MIR fiber lasers are based on different saturable absorbers (SAs) such as semiconductor saturable absorption mirrors (SESAMs), Fe^{2+}:ZnSe crystals, two-dimensional materials including graphene, topological insulators (TIs), black phosphorus (BP), and transition metal dichalcogenides (TMDs). SESAM is generally one of the most prevalent commercial SAs due to its excellent performance, and the well-developed semiconductor manufacturing techniques allow customizations of the SA parameters such as modulation depth and non-saturable loss. We have demonstrated a SESAM-based 34 nm wavelength-tunable mode-locked fiber laser operating in the 3 μm MIR spectral region [6]. However, a complex fabrication process with a considerably high cost is required for the bottom distributed Bragg reflector (DBR) in SESAM to reduce its response time [7]. Moreover, the operating bandwidth of SESAM is limited by the bottom DBR section, which makes it unsuitable for widely tunable pulsed lasers [8]. Fe^{2+}:ZnSe crystal has been widely used in MIR laser pulse generation due to its large saturable absorption cross section, small saturation energy, and high damage threshold (~2 J/cm^2) [9–11]. Recently, we have achieved a high-power, widely tunable Q-switched MIR fiber laser with 90 nm tuning range based on a Fe^{2+}:ZnSe crystal [12]. However, the bulk structure of Fe^{2+}:ZnSe is not desirable in compact and cost-effective all-fiber lasers. In the family of 2D materials, graphene, characterized by having zero bandgap, has been widely used in pulsed fiber lasers operating from the near-infrared to MIR spectral region [13–15]. Nevertheless, the low modulation depth resulting from its weak absorption restrains its application in fiber lasers [16]. Another 2D material is TI, which has a narrow bandgap and a gapless metallic state in its surface. Since Bernard *et al.* first demonstrated the feasibility of TI-based SA in 2012 [17], a few studies on pulsed fiber lasers at 1–3 μm using TI as the SA have been conducted [18–21].

However, its complex preparation process and indirect bulk band gap limit its applications. BP also shows a broadband saturable absorption in the 3 μm MIR region [22,23], but the challenge is that it is easily oxidized when exposed to air. Recently, TMDs have been extensively investigated as SAs [24–26] due to their tunable bandgaps, high third-order optical nonlinear susceptibility, ultrafast carrier dynamics, and natural abundance. Nevertheless, the TMDs require complex control of defects when serving as SAs in the MIR spectral region.

During the last decade, single-walled carbon nanotube (SWCNT)-based SAs have been drawing great attention due to their unique advantages of broad absorption bandwidth, high optical damage threshold, ultrafast response, chemical stability, and simple fabrication [27]. Besides, the band gap of a SWCNT depends on its diameter and chirality, which makes SWCNT an ideal broadband SA for wavelength-tunable fiber lasers. Pulsed fiber lasers with wavelength tunability have been demonstrated in the 1–2 μm near-infrared spectral region [28–31]. However, to the best of our knowledge, the SWCNT's saturable absorption property and potential as a wideband SA in pulsed fiber lasers operating beyond 2 μm have not yet been investigated.

In this work, we experimentally demonstrate, for the first time to our knowledge, a widely tunable, Q-switched Ho^{3+}/Pr^{3+}-codoped ZrF_4-BaF_2-LaF_3-AlF_3-NaF (ZBLAN) fiber laser using a SWCNT SA. The wavelength tuning is achieved by rotating a plane ruled grating in the oscillator. The broadband absorption of the SWCNT SA allows a continuous wavelength tuning range of 55 nm from 2837.6 to 2892.6 nm in a stable Q-switching regime. Q-switched pulses with the maximum pulse energy of 0.43 μJ are obtained with a corresponding shortest pulse duration of 1.46 μs.

2. PREPARATION AND CHARACTERIZATIONS OF A SWCNT SA

The SWCNTs were prepared with the catalytic chemical vapor deposition (CVD) method provided by a commercial supplier (Nanjing XFNANO Materials Tech Co., Ltd). The SWCNT powders were first dispersed in ethanol solvent and then sonicated for 1 h at room temperature. The top 60% of the prepared mixture was collected for experimental use. Then we dropped the mixture on a gold mirror to form a SWCNT SA. The transmission electron microscope (TEM) images of our SWCNT sample at different scales were captured with a TEM (JEM-2100F) as shown in Figs. 1(a) and 1(b). The diameters of the SWCNTs vary from 1.4 to 1.7 nm, corresponding to absorptions in the 3 μm MIR region [32]. The ranged diameter also facilitates broadband operations with enhanced modulation depth [28]. The measured Raman spectrum of the SWCNT sample using an excitation wavelength of 514 nm is depicted in Fig. 1(c). The obtained spectrum clearly shows typical CNT modes (RBM: radial breathing modes, D: disorder mode, and G: tangential mode) [29]. The relatively high ratio of G and D mode peaks confirms that the fabricated films are clean and contain few structural defects. Figure 2(a) shows the linear transmission spectrum of our SWCNT SA in the range from 2835 to 2895 nm characterized by a homemade

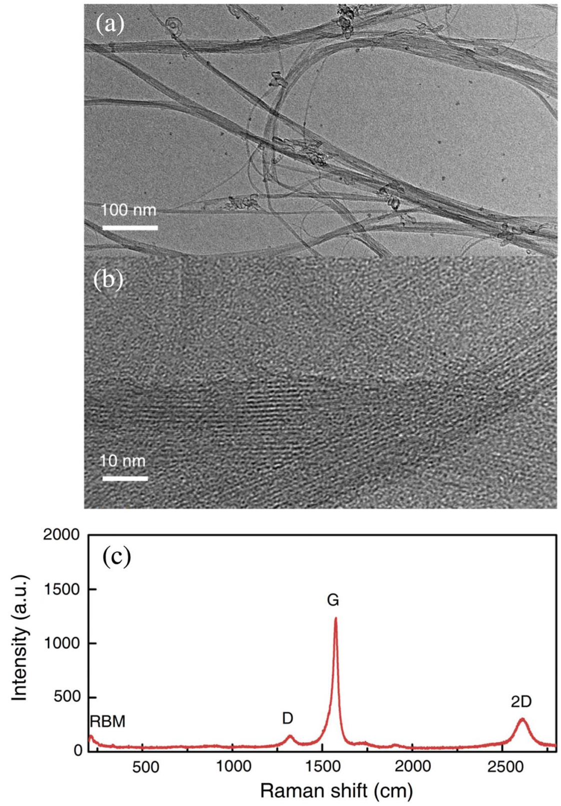

Fig. 1. TEM images of SWCNTs on the scale of (a) 100 nm and (b) 10 nm. (c) Raman spectrum.

tunable MIR fiber laser. It is shown in Fig. 2(a) that the SWCNT SA exhibits a relatively high absorption in the measured wavelength range, which is helpful for maintaining good modulation depth. By using a homemade 2850 nm mode-locked fiber laser with a repetition rate of 10.2 MHz and pulse duration of 22 ps as the laser source, we also measured the nonlinear transmission of our SWCNT SA through a typical power-dependent measurement setup based on a balanced twin detector system, which has been elaborated in previous works [21,24]. To obtain the parameters of our SWCNT SA, the transmission is fitted by a simple model of $T(I) = 1 - \Delta T \cdot \exp(-I/I_{sat}) - T_{ns}$, where $T(I)$ is the power-dependent transmission, I is the incident intensity, ΔT is the modulation depth, T_{ns} is the non-saturable loss, and I_{sat} is the saturation peak intensity. Figure 2(b) shows the nonlinear absorption curve of the SWCNT SA for 2850 nm excitation. It can be seen from Fig. 2(b) that our SWCNT SA shows nonlinear properties with the saturation peak intensity I_{sat}, modulation depth ΔT, and non-saturable loss T_{ns} of 1.66 MW/cm^2, 16.5%, and 71.8%, respectively.

3. EXPERIMENTAL SETUP

The schematic of the tunable Q-switched Ho^{3+}/Pr^{3+}-codoped ZBLAN fiber laser based on a SWCNT SA is depicted in Fig. 3. We used a 9 m long Ho^{3+}/Pr^{3+}-codoped (3 mol.% Ho^{3+}, 0.25 mol.% Pr^{3+}) ZBLAN fiber (FiberLabs Inc.) as the gain fiber with a core diameter of 10 μm and a numerical

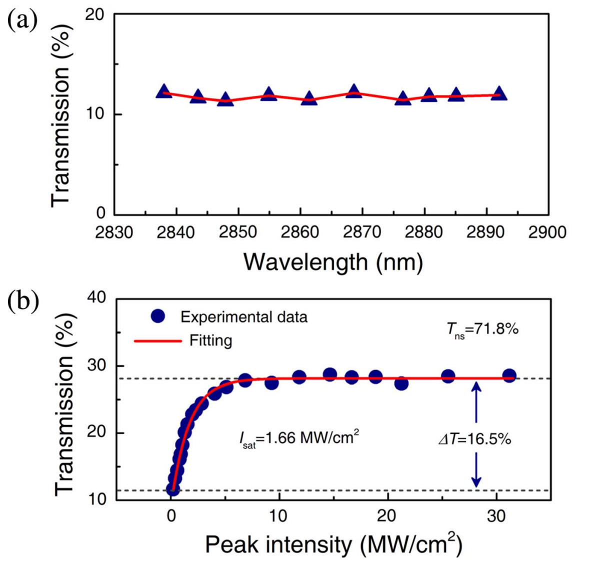

Fig. 2. (a) Linear and (b) nonlinear transmission of the SWCNT sample.

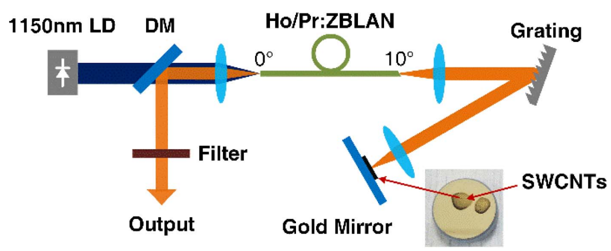

Fig. 3. Schematic setup of the tunable carbon nanotube Q-switched Ho^{3+}/Pr^{3+}-codoped ZBLAN fiber laser.

aperture (NA) of 0.2. The fiber was pumped through a CaF_2 plano-convex lens (focal length: 20 mm) by a commercial laser diode (Eagleyard Photonics) operating at 1150 nm. The front fiber end was cleaved perpendicularly to the axis of the fiber to provide ~4% feedback, while the other end of the fiber was angle-cleaved at 10° to suppress parasitic feedback. A dichroic mirror placed at a 45° angle of incidence was used as the output coupler. Two AR-coated ZnSe objective lenses (focal length: 6 mm) were used to collimate and focus the light from the angle-cleaved fiber end onto the SWCNT-coated gold mirror with a beam spot diameter of ~60 μm, which functioned as a SA and also terminated cavity feedback. As shown in Fig. 3, the SWCNTs on the gold mirror formed an approximately circular spot with a diameter of around 6 cm, corresponding to an area of 28 cm^2. The wavelength tunability was provided by rotating a plane ruled grating (450 lines/mm, blazed at 3.1 μm, 88%–91.5% reflectivity at 2.8–2.9 μm) placed between two AR-coated ZnSe objective lenses. The average power of the output laser beam was measured with a power meter (Laserpoint) along with an IR bandpass filter (Thorlabs, FB2750-500). The pulse train was captured by an InAs detector with a response time of ~2 ns connected to a 500 MHz bandwidth digital oscilloscope. The radio frequency (RF) spectrum was measured by a RF spectrum analyzer (YIAI, AV4033A). The optical spectrum was analyzed by a monochromator with a scanning resolution of 0.1 nm (Princeton Instrument Acton SP2300).

4. RESULTS

First, we tuned the grating at a fixed angle to maximize the output power. A stable passively Q-switched pulse train was observed as the launched pump power increased to 186.1 mW. This stable Q-switched pulse train could be maintained with the launched pump power increased to 445.6 mW. A stable pulse train with a duration of 1.46 μs and repetition rate of 131.6 kHz at the maximum launched pump power of 445.6 mW is shown in Fig. 4. The left inset of Fig. 4 shows the corresponding optical spectrum. The central wavelength is 2853.0 nm, and the 3 dB bandwidth is 1.4 nm. The right inset is the measured RF spectrum at a resolution bandwidth of 100 Hz in a 45 kHz scanning span. The peak is located at 131.6 kHz, and the signal-to-noise ratio is over 40 dB, indicating a stable Q-switching regime. With the increasing launched pump power at this fixed wavelength of 2853.0 nm, we also recorded the evolutions of the pulse properties. Figure 5(a) displays the repetition rate and pulse duration versus the launched pump power. As the launched pump power grows from 186.1 to 445.6 mW, the repetition rate is increased from 83.3 to 131.6 kHz, and the pulse duration is narrowed from 2.40 to 1.46 μs. As shown in Fig. 5(b), we also measured the output power and calculated the single pulse energy at the varied launched pump powers. It is observed that both output power and single pulse energy are linearly increased with the increasing of the launched pump power. At the launched pump power of 445.6 mW, we achieved the maximum output power and pulse energy of 55.8 mW and 0.43 μJ, respectively.

By finely rotating the kinematic mount holding the grating, we investigated the wavelength tunability of this Q-switched laser at a fixed moderate pump power of 401.5 mW. As shown in Fig. 6, a tuning range of 55 nm, covering the central wavelength from 2837.6 to 2892.6 nm, is obtained with the current laser setup, and the stable Q-switching operation can be

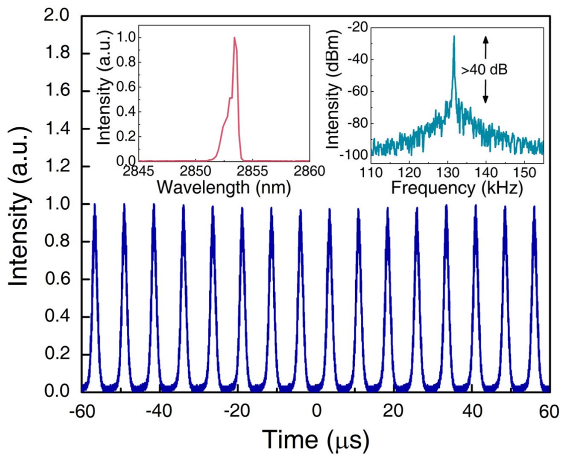

Fig. 4. Q-switched pulse train at the launched pump power of 445.6 mW. Inset: corresponding optical and RF spectra.

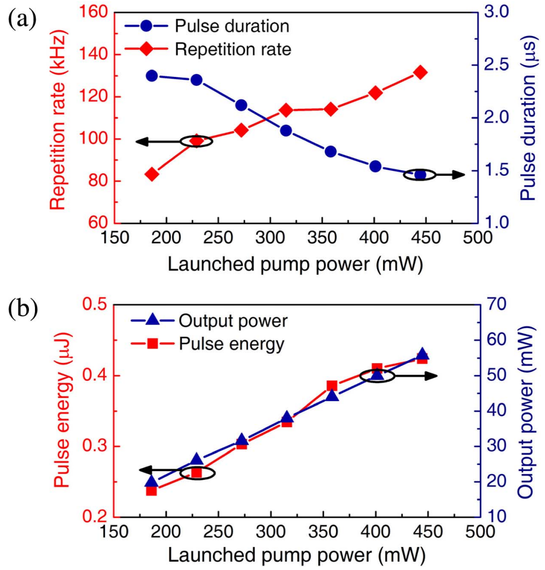

Fig. 5. (a) Repetition rate and pulse duration, (b) output power and single pulse energy as functions of the launched pump power.

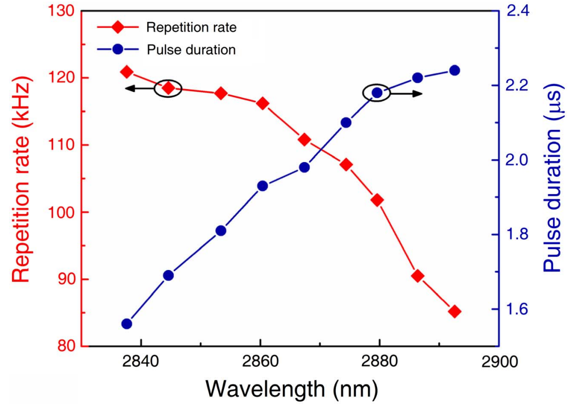

Fig. 7. Repetition rate and pulse duration as functions of the tuning wavelength.

maintained within the entire tuning range. The tunable range is mainly limited by the high intracavity loss and the gain spectrum of the Ho^{3+}/Pr^{3+}-codoped ZBLAN fiber rather than the SWCNT SA. For example, when we set the launched pump power to 326.7 mW, the tuning range narrowed to 43.2 nm (from 2839.2 to 2882.4 nm). This is because the reduced intracavity energy in wavelength regions beyond the 43.2 nm tuning range became insufficient to maintain the *Q*-switched operation. Thus, we believe that the tuning range could be further broadened with an optimized cavity and higher pump power using our current SWCNT SA. The average output power as a function of the tuning wavelength is also given in Fig. 6. The output power increases initially and then decreases with the extension of the lasing wavelength, which matches well with the gain profile of Ho^{3+}/Pr^{3+}-codoped ZBLAN fiber [33]. The power difference is measured to be less than 10%. We also recorded the repetition rate and pulse duration during the tuning of the output wavelength. The repetition rate and pulse duration as functions of the output wavelength are illustrated in Fig. 7. The repetition rate decreases from 120.9 to 85.2 kHz, while the pulse duration increases from 1.56 to 2.24 μs with the output wavelength varying from 2837.6 to 2892.6 nm, as shown in Fig. 7. Combined with the output powers at different wavelengths, as shown in Fig. 6, we find that the single pulse energy varies from 0.38 to 0.54 μJ in this tuning range. We assume that this variation originates from the combination of different cavity losses, fiber gains, and varied bleaching rates of the SWCNT SA under different population depletion rates caused by different intracavity laser intensities.

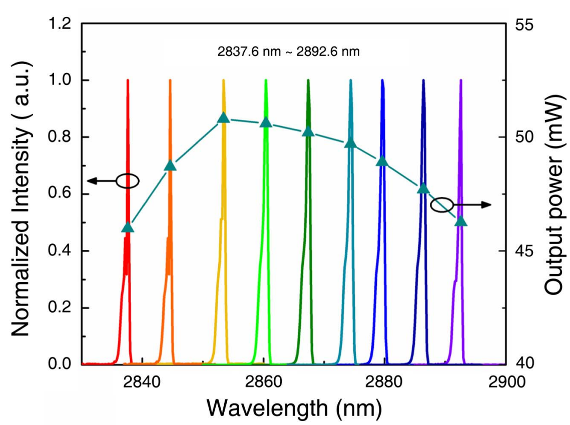

Fig. 6. Normalized spectra and the corresponding average output power from the tunable *Q*-switched laser.

5. CONCLUSION

In summary, we have demonstrated, to the best of our knowledge, the first widely tunable, passively *Q*-switched Ho^{3+}/Pr^{3+}-codoped ZBLAN fiber laser at 2.8 μm by using SWCNTs as the SA. The central wavelength of the *Q*-switched pulses could be continuously tuned across 55 nm (from 2837.6 to 2892.6 nm). Our results have verified that the SWCNT SA possessing broadband nonlinear absorption shows great potential for wavelength-tunable *Q*-switched fiber lasers in the 3 μm MIR region. The broadband and strong nonlinear absorption provided by the SWCNT SA combined with the inherent simplicity in wavelength selection by the plane ruled diffraction grating leads to robust and repeatable operation. Such SWCNT-based *Q*-switched fiber lasers with a wide MIR wavelength-tuning range can provide a reliable, simple, robust, and cost-effective solution to a wide range of both scientific and industrial applications.

Funding. National Natural Science Foundation of China (NSFC) (61875033, 61505024, 61435003, 61421002, 61705147, 61605219, 61775031); Chengdu Science and Technology Huimin Project (2016-HM01-00265-SF, 2016-HM01-00269-SF); Fundamental Research Funds for the Central Universities (YJ201723).

†These authors contributed equally to this work.

REFERENCES

1. P. Werle, F. Slemr, K. Maurer, R. Kormann, R. Mucke, and B. Janker, "Near- and mid-infrared laser-optical sensors for gas analysis," Opt. Lasers Eng. **37**, 101–114 (2002).
2. A. Godard, "Infrared (2–12 μm) solid-state laser sources: a review," C. R. Phys. **8**, 1100–1128 (2007).
3. M. Pollaun and S. D. Jackson, *Mid-Infrared Coherent Sources and Applications* (Springer, 2008).
4. K. Ke, C. Xia, M. N. Islam, M. J. Welsh, and M. J. Freeman, "Mid-infrared absorption spectroscopy and differential damage in vitro between lipids and proteins by an all-fiber-integrated supercontinuum laser," Opt. Express **17**, 12627–12640 (2009).
5. M. Vainio, M. Merimaa, and L. Halonen, "Frequency-comb-referenced molecular spectroscopy in the mid-infrared region," Opt. Lett. **36**, 4122–4124 (2011).
6. C. Wei, H. Shi, H. Luo, H. Zhang, Y. Lyu, and Y. Liu, "34 nm-wavelength-tunable picosecond Ho^{3+}/Pr^{3+}-codoped ZBLAN fiber laser," Opt. Express **25**, 19170–19178 (2017).
7. U. Keller, K. J. Weingarten, F. X. Kartner, D. Kopf, B. Braun, I. D. Jung, R. Fluck, C. Honninger, N. Matuschek, and J. A. der Au, "Semiconductor saturable absorber mirrors (SESAMs) for femtosecond to nanosecond pulse generation in solid-state lasers," IEEE J. Sel. Top. Quantum Electron. **2**, 435–453 (1996).
8. D. Kopf, A. Prasad, G. Zhang, M. Moser, and U. Keller, "Broadly tunable femtosecond Cr:LiSAF laser," Opt. Lett. **22**, 621–623 (1997).
9. A. A. Voronov, V. I. Kozlovskii, Y. V. Korostelin, A. I. Landman, Y. P. Podmarkov, V. G. Polushkin, and M. P. Frolov, "Passive Fe^{2+}:ZnSe single-crystal *Q* switch for 3-μm lasers," Quantum Electron. **36**, 1–2 (2006).
10. J. Li, H. Luo, L. Wang, B. Zhai, H. Li, and Y. Liu, "Tunable Fe^{2+}:ZnSe passively *Q*-switched Ho^{3+}-doped ZBLAN fiber laser around 3 μm," Opt. Express **23**, 22362–22370 (2015).
11. C. Wei, X. Zhu, R. A. Norwood, and N. Peyghambarian, "Passively continuous-wave mode-locked Er^{3+}-doped ZBLAN fiber laser at 2.8 μm," Opt. Lett. **37**, 3849–3851 (2012).
12. C. Wei, H. Zhang, H. Shi, K. Konynenbelt, H. Luo, and Y. Liu, "Over 5-W passively *Q*-switched mid-infrared fiber laser with a wide continuous wavelength tuning range," IEEE Photon. Technol. Lett. **29**, 881–884 (2017).
13. C. Wei, X. Zhu, F. Wang, Y. Xu, K. Balakrishnan, F. Song, R. A. Norwood, and N. Peyghambarian, "Graphene *Q*-switched 2.78 μm Er^{3+}-doped fluoride fiber laser," Opt. Lett. **38**, 3233–3236 (2013).
14. G. Zhu, X. Zhu, F. Wang, S. Xu, Y. Li, X. Guo, K. Balakrishnan, R. A. Norwood, and N. Peyghambarian, "Graphene mode-locked fiber laser at 2.8 μm," IEEE Photon. Technol. Lett. **28**, 7–10 (2015).
15. G. Zhu, X. Zhu, K. Balakrishnan, R. A. Norwood, and N. Peyghambarian, "Fe^{2+}:ZnSe and graphene *Q*-switched singly Ho^{3+}-doped ZBLAN fiber lasers at 3 μm," Opt. Mater. Express **3**, 1365–1377 (2013).
16. R. R. Nair, P. Blake, A. N. Grigorenko, K. S. Novoselov, T. J. Booth, T. Stauber, N. M. R. Peres, and A. K. Geim, "Fine structure constant defines visual transparency of graphene," Science **320**, 1308 (2008).
17. F. Bernard, H. Zhang, S. P. Gorza, and P. Emplit, "Towards mode-locked fiber laser using topological insulators," in *Nonlinear Photonics* (2012), paper NTh1A.5.
18. Z. Q. Luo, Y. Huang, J. Weng, H. Cheng, Z. Lin, B. Xu, Z. Cai, and H. Xu, "1.06 μm *Q*-switched ytterbium-doped fiber laser using few-layer topological insulator Bi_2Se_3 as a saturable absorber," Opt. Express **21**, 29516–29522 (2013).
19. Z. Yu, Y. Song, J. Tian, Z. Dou, H. Guoyu, K. Li, H. Li, and X. Zhang, "High-repetition-rate *Q*-switched fiber laser with high quality topological insulator Bi_2Se_3 film," Opt. Express **22**, 11508–11515 (2014).
20. M. Jung, J. Lee, J. Koo, J. Park, Y. Song, K. Lee, S. Lee, and J. Lee, "A femtosecond pulse fiber laser at 1935 nm using a bulk-structured Bi_2Te_3 topological insulator," Opt. Express **22**, 7865–7874 (2014).
21. J. Li, H. Luo, L. Wang, C. Zhao, H. Zhang, H. Li, and Y. Liu, "3-μm mid-infrared pulse generation using topological insulator as the saturable absorber," Opt. Lett. **40**, 3659–3662 (2015).
22. Z. Qin, G. Xie, H. Zhang, C. Zhao, P. Yuan, S. Wen, and L. Qian, "Black phosphorus as saturable absorber for the *Q*-switched Er:ZBLAN fiber laser at 2.8 μm," Opt. Express **23**, 24713–24718 (2015).
23. Z. Qin, G. Xie, C. Zhao, S. Wen, P. Yuan, and L. Qian, "Mid-infrared mode-locked pulse generation with multilayer black phosphorus as saturable absorber," Opt. Lett. **41**, 56–59 (2016).
24. C. Wei, H. Luo, H. Zhang, C. Li, J. Xie, J. Li, and Y. Liu, "Passively *Q*-switched mid-infrared fluoride fiber laser around 3 μm using a tungsten disulfide (WS_2) saturable absorber," Laser Phys. Lett. **13**, 105108 (2016).
25. R. I. Woodward, E. J. R. Kelleher, R. C. T. Howe, G. Hu, F. Torrisi, T. Hasan, S. V. Popov, and J. R. Taylor, "Tunable *Q*-switched fiber laser based on saturable edge-state absorption in few-layer molybdenum disulfide (MoS_2)," Opt. Express **22**, 31113–31122 (2014).
26. Y. Huang, Z. Luo, Y. Li, M. Zhong, B. Xu, K. Che, H. Xu, Z. Cai, J. Peng, and J. Weng, "Widely-tunable, passively *Q*-switched erbium-doped fiber laser with few-layer MoS_2 saturable absorber," Opt. Express **22**, 25258–25266 (2014).
27. A. Martinez and Z. Sun, "Nanotube and graphene saturable absorbers for fibre lasers," Nat. Photonics **7**, 842–845 (2013).
28. F. Wang, A. G. Rozhin, V. Scardaci, Z. Sun, F. Hennrich, I. H. White, W. I. Milne, and A. C. Ferrari, "Wideband-tuneable, nanotube mode-locked, fibre laser," Nat. Nanotechnol. **3**, 738–742 (2008).
29. Y. Meng, Y. Li, Y. Xu, and F. Wang, "Carbon nanotube mode-locked thulium fiber laser with 200 nm tuning range," Sci. Rep. **7**, 45109 (2017).
30. Y. S. Fedotov, S. M. Kobtsev, R. N. Arif, A. G. Rozhin, C. Mou, and S. K. Turitsyn, "Spectrum-, pulsewidth-, and wavelength-switchable all-fiber mode-locked Yb laser with fiber based birefringent filter," Opt. Express **20**, 17797–17805 (2012).
31. M. Chernysheva, A. Rozhin, Y. Fedotov, C. Mou, R. Arif, S. M. Kobtsev, E. M. Dianov, and S. K. Turitsyn, "Carbon nanotubes for ultrafast fibre lasers," Nanophotonics **6**, 1–30 (2017).
32. S. Reich, C. Thomsen, and J. Maultzsch, *Carbon Nanotubes: Basic Concepts and Physical Properties* (Wiley, 2004).
33. D. Hudson, E. Magi, L. Gomes, and S. D. Jackson, "1 W diode-pumped tunable Ho^{3+}, Pr^{3+}-doped fluoride glass fibre laser," Electron. Lett. **47**, 985–986 (2011).